Proceedings of 10th International Conference on Precision, Meso, Micro and Nano Engineering (COPEN 10)
December 07 – 09, 2017, Indian Institute of Technology Madras, Chennai – 600 036 INDIA

Electro-Polishing of Hypodermic Needles and its Influence on Needle-Tissue Interaction Forces

Ramesh Kuppuswamy[a], Mubita Kapui[a]
[a]Advanced Manufacturing Laboratory, Department of Mechanical Engineering
University of Cape Town, SOUTH AFRICA – 7701

Abstract

Hypodermic needles are useful when percutaneous diagnosis or treatment is required. The advent of surgical robots on minimally invasive treatment of cancer such as radio frequency ablation (RFA) and percutaneous ethanol injection treatment (PEIT) necessitate an understanding of needle-tissue interface mechanics. Pats research has been done regarding needle insertion forces and tissue deformation for a variety of tissues. It is understood that the main factors affecting insertion accuracy are needle deflection and tissue deflection. Hypodermic needle deflection is attributed to the needle geometry and the mechanical properties of the tissue. Tissue deflection is the result of a combination of the needle tip contact force, mechanical properties of the tissue and frictional forces between the needle shaft and tissue. Tissue deflection makes percutaneous treatments difficult as the area being targeted for treatment shifts as the tissue is deformed. The present research aims to reduce needle tip contact force and frictional forces by applying a controlled electro-polishing process. Electro-polishing is an electrochemical material removal process. It is usually used to substitute mechanical polishing as a means of obtaining smooth surfaces. When applied to stainless steel, it produces smooth, clean surfaces with improved corrosion resistance. These properties make the electro-polishing process ideal for biomedical applications. While electro-polishing does have a number of advantages over mechanical polishing, it is difficult to control and thus consistent results are difficult to obtain. This is mainly the result of the composition of the electrolyte used for electro-polishing. Electrolytes composed of sulphuric and phosphoric acids of varying compositions and concentrations are usually used to electro-polish stainless steels. In the present research, hypodermic needles of material stainless steel 304 were electro-polished with electrolytes of varying compositions of sulphuric and phosphoric acids. Various combinations of both volume ratios and concentrations were used until an electrolyte producing consistent results was obtained. Force data was then be obtained for both standard and electro-polished needles by making use of silicone phantoms as tissue substitutes. It was found that the electrolyte producing the most consistent electro-polishing results was a mixture of H2O, H2SO4 (98%) and H3PO4 (85%) at a volume ratio of 2:3:5. It was observed that the material removed during the electro-polishing process could be controlled to an error estimate of 6%. The surfaces obtained showed improved cleanness and reduced surface roughness (Ra). The forces during insertion were less for the electro-polished needles with the most consistent results obtained at a current density of 0.66 A/cm^2. A needle tissue interaction force model was developed and verified with extensive experiments. It was shown that electro-polishing has a sharpening effect on the needles and results in a reduction in the coefficient of friction at the needle-phantom interface.

Keywords: Electro-polishing, Hypodermic Needle, Needle-Tissue Interaction

1. INTRODUCTION

Hypodermic needles are useful when percutaneous diagnosis or treatment is required. The advent of surgical robots and minimally invasive treatment of cancer such as radio frequency ablation (RFA) and percutaneous ethanol injection treatment (PEIT) necessitate an understanding of needle insertion mechanics [1,2]. Moreover, the pain experienced during needle insertion is dependent on the maximum forces exerted during the process. A reduction in the pain experienced during needle insertion would reduce the phobia associated with the process over time [3]. In recent years, research has been done regarding needle insertion forces and tissue deformation for a variety of tissues [4-7]. It is understood that the main factors affecting insertion accuracy are needle deflection and tissue deflection. Needle deflection is attributed to the needle geometry and the mechanical properties of the tissue. Tissue deflection is the result of a combination of the needle tip contact force, mechanical properties of the tissue and frictional forces between the needle shaft and the tissue [8]. A past research reveals a developed device for the electro-polishing of drilled surgical needles. The removal of surface protrusions and defects such as burrs reduces tissue trauma during needle insertion [9]. In general, when a force is applied to the needle while it is in contact with the tissue surface, the surface is deformed before it is punctured by the needle tip. The viscoelastic nature of biological tissues was modelled using different combinations of linear springs and dampers. The most common models used in literature are the Maxwell, Voigt and Kelvin models [10]. Previous attempt also suggests the consideration of the non-linear nature of the tissue viscoelasticity at larger displacements. After the tissue has been punctured, cutting and friction forces begin to act on the needle in addition to the force due to the tissue stiffness. The stiffness force continues to act because the tissue ahead of the needle bevel continues to be compressed as the needle moves through the tissue. The cutting force acts along the needle cutting edge and increases as more of the cutting edge enters the tissue. It then maintains a constant value when the whole of the cutting edge is inside the tissue. The friction force acts on the needle bevel and shaft. It increases with the increase in surface area of the needle which is in contact with the tissue [11]. A pig liver was used and the aim was to characterize soft tissue properties for haptic display during surgery. Also, a study on cutting forces was noted by making use of the concept of elementary cutting tool (ECT) edges [12]. The friction force acting on the needle is a combination of both coulomb friction and viscous friction. It is affected by a number of factors such as: the needle surface texture, the surface wettability, the mechanical properties of the tissue and the needle insertion speed. Another important factor is the real area of contact between the asperities on the needle surface and the tissue as it is directly related to the total friction force at the needle-tissue interface. The real area of contact is in turn dependent on the surface texture and needle surface area. The wettability of the needle surface plays a role because a

ISBN: 978-93-80689-28-9

more hydrophilic surface ensures that there is less solid contact between the needle surface asperities and the tissue. Past findings showed that more hydrophilic surfaces exhibit lower coefficients of friction in aqueous environments [13]. Several past research tabulates the various friction and friction models on needle-tissue interactions [14]. Friction force was also modelled based on the relative velocity between the needle and the tissue and the findings reveals that the friction force increases with an increase in velocity [15]. Another research reveals the effectiveness of needle rotation on the friction force and the results suggest that the friction force reduces for all the different rotations employed [16]. A detailed FE analysis model the insertion forces when a needle is inserted into a soft silicone phantom. The model has considered the silicone phantom as a hyper-elastic material [17]. Both static and kinetic friction were included in their simulations. The simulation results were found to have the same shape for the range of their experiment data. Another FE research unveils the needle-gelatine phantom behavior. This research has fracture mechanics approach by making use of cohesive elements [18]. A penalty-based cohesive-zone approach was used to model the creation and propagation of the crack created by the needle tip. The only parameter required was the strain energy release rate of the crack. The parameters varied during their simulations were the coefficient of friction and the penalty parameters of the cohesive zone. Their final simulation results showed a good fit to the experiment data [19]. Also, a past study determines the effect of different needle insertion angles on the stresses and deformations induced in the femoral tissue during femoral vein catheterization. From their simulation results, they found that the needles injected at an angle of 90^o experienced the lowest stresses and deformations [20]. The effects of tissue rupture toughness, tissue elasticity and needle bevel angle on the needle tip forces during needle insertion was also unveiled. It was also established that local effective modulus (LEM) was constant for each insertion speed and concluded that the properties of the tissue did not vary much as the needle insertion depth changed. However no prior research was apparently seen on the effect of needle polishing on the needle-tissue interaction forces. Therefore, an attempt was made to reduce the needle tip contact force and frictional forces between the needle shaft and the tissue by applying a controlled electro-polishing process.

2. NEEDLE INSERTION FORCE MODEL

An analytical force model was developed based on the change in surface area and surface texture of the hypodermic needles after electro-polishing. Electro-polishing results in the removal of material from the hypodermic needle surfaces and the process has two main effects; improvement of the surface finish and thinning of the needle wall. In general, the surface spectrum of the needle could be expressed as sinusoidal profile as given in equation 1.

$$h(x) = R_a Sin\left(\frac{2\pi}{\lambda}x\right) \quad (1)$$

Where h is the vertical displacement of the surface from the mean at a given position (x). R_a is the arithmetic mean roughness and λ is the wavelength of the profile. The needle insertion force was modelled to reflect the different events during needle insertion. They are (see Fig.1A);

- Needle in progression to full contact with phantom before penetration and hence force due to tissue stiffness acts predominantly $0 \le x \le x_1$
- Needle penetrate into `the phantom and increase the friction and cutting force acting on the needle $x_1 \le x \le x_2$
- Needle tip exits the phantom and hence the force due to tissue stiffness and cutting reduces as the cutting edge exits the phantom $x_2 \le x \le x_3$

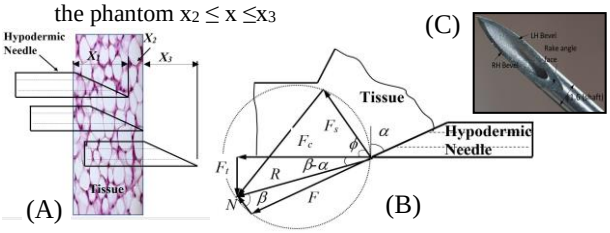

Fig. 1. A) Stages of needle advancement on Tissue; B) Needle-Tissue interface diagram; C) Needle geometry details

The needle-tissue interaction force was modelled based on an influence of surface texture conditions of the hypodermic needle. The hypodermic needle-tissue interface force signature was explained using the merchant circle diagram as shown in Fig. 1 B. Using the merchant circle diagram the cutting force, *Fc* was given as;

$$F_C = R\cos(\beta-\alpha) = \frac{\omega t_o \tau \cos(\beta-\alpha)}{\sin(\phi)\cos(\phi+\beta-\alpha)} \quad (2)$$

where R= Resultant force; α = rake angle (45°); β= Friction angle; ϕ=shear angle; ω= width of cut (equated to the diameter of the hypodermic needle); t_o= depth of penetration (equated to $(l/\cos(\alpha))$ where l = cutting edge length of the needle and τ= cutting resistance of the tissue.

Equation 2 is re-written by introducing the cutting-edge length of the needle as;

$$F_C = R\cos(\beta-\alpha) = \frac{\omega l \tau \cos(\beta-\alpha)}{\cos(\alpha)\sin(\phi)\cos(\phi+\beta-\alpha)} \quad (3)$$

The product cutting edge length of the needle and width is equated to the contact area of needle-tissue interface which is expected to vary at various electropolishing conditions. The contact area of the needle-tissue is computed as follows;

Prior to electropolishing the needle surface was generated by the grinding process and the profiles is shown in Fig. 2A. The electropolishing process would tend to flatten the peak a and a typical profile obtained after the electropolishing is shown in Fig.2B [21]. The radius of the surface profile of the needle is equated surface finish, R_a value and hence the total surface area (A) for a unit area is given as;

$$A = n((2\pi R_a^2) + (\lambda - 2R_a)(\lambda - 2R_a)) \quad (4)$$

where n = number of surface indentation for a given a unit area; R_a = surface finish average value; λ = wavelength of the surface profile

Fig. 2. A typical needle surface profile A) before polishing; B) after Electro-polishing

Combining equation 3 and 4, the equation 3 is rewritten for a unit area of the needle as;

$$F_C = R\cos(\beta-\alpha) = \frac{(n)((2\pi R_a^2) + (\lambda - 2R_a)(\lambda - 2R_a))\tau\cos(\beta-\alpha)}{\sin(\phi)\cos(\phi+\beta-\alpha)} \quad (5)$$

The shear angle was computed assuming that the friction between the needle -tissues = 0.663 and cutting ratio = 1 [14]. Upon applying the needle-tissue geometry and the surface texture of the needle, the theoretical values of F_c were

computed. Shown in Fig. 3 is the theoretical values of F_c for the various electropolishing conditions.

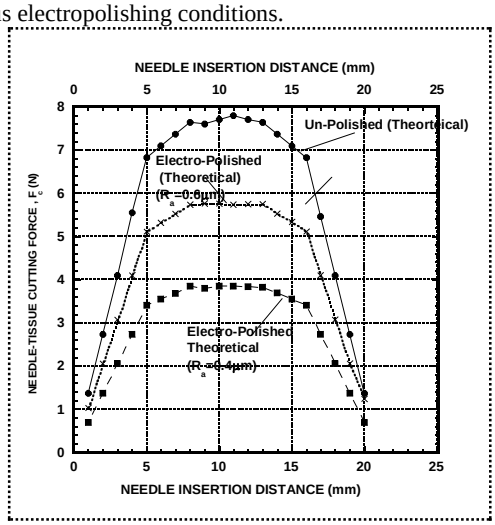

Fig.3. Needle-Tissue Cutting force behavior for the various electro-polishing conditions

3. EXPERIMENTAL SET-UP

The hypodermic needle was connected to the anodic (+) side of a direct current power supply, and the cathodic (-) side is connected to a stainless steel (SS304) electrode for facilitating the electro-polishing process. Both the hypodermic needle and the cathode are immersed in an electrolyte which is a mixture of H_2O, H_2SO_4 (98%) and H_3PO_4 (85%) at a volume ratio of 2:3:5. A Lodestar 8203 DC power supply of voltage 2 to 20 V was applied for the experiments. Shown in Fig.4 is a photo of the developed set up. Before the electro-polishing experiments, the hypodermic needles were cleaned using the ethanol and de-ionized water.

Fig. 4. Experimental set up for electropolishing the Hypodermic needle

4. RESULTS AND DISCUSSION

The electropolished experimental findings of the hypodermic needle was further modelled for the different electro-polishing conditions and shown in Fig. 5. The results suggest that a current and electropolishing time of value 1~1.5A and 10~15 minutes would impart a surface finish of value 0.2~0.3 μm. It is widely accepted that four different mechanisms take place on electropolishing of the needles such as: oxidation, passivation, diffusion limited current and oxygen evolution. At a current of 0.82A, the surface texture was observed to improve in an almost linear fashion. The highest reduction in surface roughness occurred at a current of 0.93A and time of 10 minutes with a polishing percentage of 64.7 %. The most consistent results were obtained at current 0.93A. Shown in Fig. 6 is the SEM micrographs of the needle for the different electro-polishing parameters. It is observed that the bevel surface of the standard needle has more scratches, striations and foreign particles than any of the electro-polished needles. The needle walls are observed to thin as the electro-polishing parameters are increased. At an electro-polishing current density of 0.16 A/cm^2, there is a decrease in the prominence of the striations on the bevel surface with increased electro-polishing time. The same trend is observed at the higher current densities with the needle electro-polished at J = 0.66 A/cm^2 and t = 5 mins showing a improved surface texture. The smoother and cleaner surfaces reduce the amount of friction present at the needle-tissue interface during needle insertion. The reduction in needle-tissue contact area resulted in reduced cutting forces during needle insertion. While the needle tips show improvement with increased electro-polishing current and time, the maximum useable parameters are limited by the small mass of the hypodermic needles. However, the removal of too much material from the needle surface results in the rupturing of the needle wall.

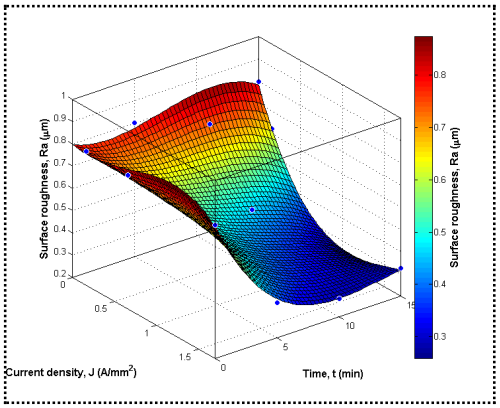

Fig.5. Influence of electropolishing parameters on needle surface texture

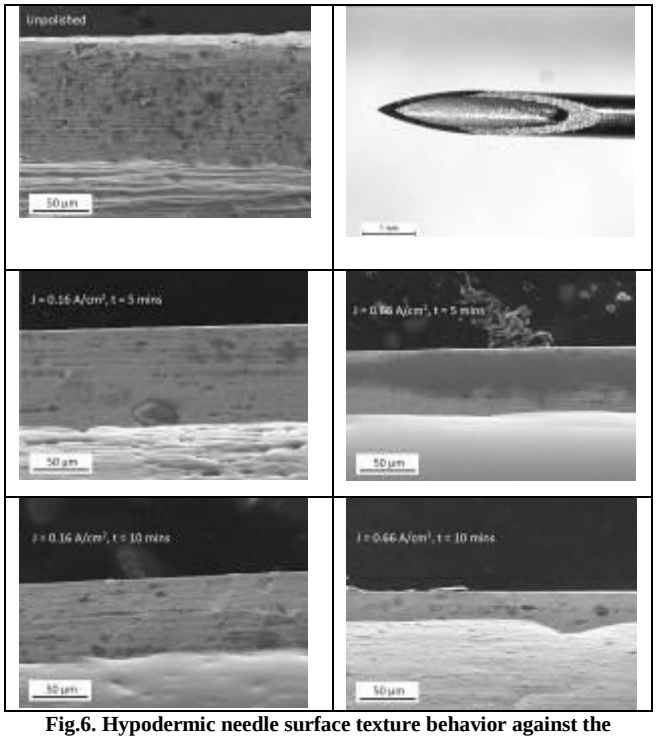

Fig.6. Hypodermic needle surface texture behavior against the electropolishing conditions

The hypodermic needle insertion force data was captured for an insertion speed of 2000 mm/min. Shown in Fig. 7 is the needle

insertion force plot against the insertion depth. The force profiles show how the geometry of the needle such as: shaft, needle point and bevel affects the insertion forces as the needle surfaces interacts with the phantom during insertion. The cutting action is performed by the needle tip and the cutting edges along the bevel. The main source of friction is the surface asperities on the needle shaft. The electro-polishing process reduces the needle surface contact area as the process removes material on an ion by ion basis and leaves a smooth, clean surface. While the mechanism of the electro-polishing process is such that it attacks sharp points preferentially, the needle is not blunted by it, instead it is sharpened. This happens because the process attacks both the inside and outside surfaces of the needle. This creates sharper cutting edges as the needle wall is thinned even more at the edges and needle tip. The unpolished needle has exhibited a maximum force of magnitude 5 to 6.8 N while the needle was inserted at speed 2000 mm/min. After electropolishing at a current of 0.66 A/cm^2 the maximum needle-tissue interaction force has reduced to 4~5.4 N and 3.6~4.5 N for a polishing time of 5 minutes and 10 minutes respectively. The results conclude that the electropolished needle has enabled to reduce the needle-tissue interaction force by 14.9 % ~23.7 %.

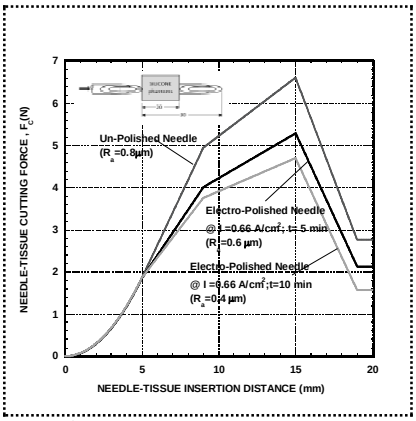

Fig.7: Influence of electropolishing conditions on the needle-tissue interaction forces

5. CONCLUSION

The effects of the electro-polishing current, time and the needle insertion speed on the cutting forces during needle insertion were investigated. The results indicated that the electro-polishing current had a much larger effect than the parameter polishing time. The insertion force experiments showed that all the electro-polished needles also showed reduced insertion forces compared to the unpolished needle. Furthermore, the electro-polishing has a sharpening effect on the needles and results in a reduction in the coefficient of friction at the needle-phantom interface.

ACKNOWLEDGMENTS

The authors wish to thank Mr. Horst Emrich (University of Cape Town, Cape Town, South Africa) for the support rendered on the electro-polishing experiments. This project was supported by fund NRF GRANT: INCENTIVE FUNDING FOR RATED RESEARCHERS (IPRR) –South Africa through Reference: IFR150204113619 and Grant No: NRF-96066.

References

1. Kobayashi.Y., Development of an integrated needle insertion system with image guidance and deformation simulation, Computerized Medical Imaging and Graphics, 2010,34(1)9-18.

2.Koethe.Y., Accuracy and efficacy of percutaneous biopsy and ablation using robotic assistance under computed tomography guidance: a phantom study, European radiology, 2014, 24(3)723-730.

3.Haq.M., Clinical administration of micron needles: skin puncture, pain and sensation, Biomedical microdevices, 2009, 11(1)35-47.

4.Okamura.A.M., C. Simone., M.D. O'leary., Force modeling for needle insertion into soft tissue, IEEE transactions on biomedical engineering, 2004,51(10)1707-1716.

5.Misra.S., K.B. Reed., B.W. Schafer., K.T. Ramesh., A.M. Okamura, Mechanics of flexible needles robotically steered through soft tissue, The International journal of robotics research, 2010,29(13)1640-1660.

6.Barbé, L., Needle insertions modeling: identifiability and limitations, Biomedical signal processing and control, 2007, 2(3)191-198.

7. Barnett, A.C., Y.-S. Lee, J.Z. Moore, Fracture mechanics model of needle cutting tissue, Journal of Manufacturing Science and Engineering, 2016, 138(1)011005.

8. Zhao.H., A needle insertion concept and robot system for breast tumor, 2016 IEEE International Conference on Mechatronics and Automation.

9. Howard, B., Electropolishing of drilled surgical needles, US patent 3703452 A

10. Fung.Y.C., Book: Biomechanics: mechanical properties of living tissues, 2013: Springer Science & Business Media.

11. Chanthasopeephan, T., Characterization of soft tissue cutting for haptic display: Experiments and computational models, 2006, Drexel University.

12. Moore.J.Z., Blade oblique cutting of tissue for investigation of biopsy needle insertion, Trans. NAMRI, 2009, 37,49-56.

13. Borruto.A., G. Crivellone.,F. Marani., Influence of surface wettability on friction and wear tests, Wear, 1998, 222(1)57-65.

14. Van Geffen, V., A study of friction models and friction compensation, DCT, 2009, 118, 24.

15. Kobayashi, Y., T. Sato., M.G. Fujie., Modeling of friction force based on relative velocity between liver tissue and needle for needle insertion simulation, Engineering in Medicine and Biology Society, 2009, EMBC 2009.

16. Abolhassani. N., R. Patel., M. Moallem., Experimental study of robotic needle insertion in soft tissue, International Congress Series, 2004, Elsevier.

17. Cheng. Z., Modelling needle forces during insertion into soft tissue, Engineering in Medicine and Biology Society conference (EMBC), 2015

18. Oldfield. M., Detailed finite element modelling of deep needle insertions into a soft tissue phantom using a cohesive approach, Computer methods in biomechanics and biomedical engineering, 2013, 16(5)530-543.

19. Diehl. T., On using a penalty-based cohesive-zone finite element approach, Part I: Elastic solution benchmarks, International Journal of Adhesion and Adhesives, 2008. 28(4) 237-255.

20. Halabian.M., A combination of experimental and finite element analyses of needle–tissue interaction to compute the stresses and deformations during injection at different angles, Journal of clinical monitoring and computing,2016,30(6)965-975.

21. M. S. Bobji., Giridhar., Evolution of Surface Roughness During Electropolishing, Tribology Letters, 2014, 55(1)93–101.